Articles in PresS. Am J Physiol Regul Integr Comp Physiol (January 2, 2008). doi:10.1152/ajpregu.00695.2007

Differential localization and regulation of two aquaporin-1 homologs in the intestinal epithelia of the marine teleost *Sparus aurata*

Demetrio Raldúa, David Otero, Mercedes Fabra, and Joan Cerdà

Laboratory IRTA-Institute of Marine Sciences, CSIC, Passeig Marítim 37-40, 08003-Barcelona, Spain

Running title: Aquaporin-1 homologs in teleost intestine

Please, send editorial comments to: Joan Cerdà, Lab IRTA-ICM, CMIMA-CSIC, Passeig Marítim 37-49, 08003-Barcelona, Spain. Phone: +34-93 230 95 31, Fax: +34-93 230 95 55. E-mail: joan.cerda@irta.es

Address for reprint requests and other correspondence: J. Cerdà, Lab IRTA-ICM, CMIMA-CSIC, Passeig Marítim 37-49, 08003-Barcelona, Spain (E-mail: joan.cerda@irta.es)

Abstract

Aquaporin (AQP)-mediated intestinal water absorption may play a major osmoregulatory role in euryhaline teleosts, although the molecular identity and anatomical distribution of AQPs in the fish gastrointestinal tract is poorly known. Here, we have investigated the functional properties and cellular localization in the intestine of two gilthead seabream (*Sparus aurata*) homologs of mammalian aquaporin-1 (AQP1), named SaAqp1a and SaAqp1b. Heterologous expression in *Xenopus laevis* oocytes showed that SaAqp1a and SaAqp1b were water-selective channels. Real-time quantitative RT-PCR and Western blot using specific antisera indicated that abundance of SaAqp1a mRNA and protein was higher in duodenum and hindgut than in the rectum, while abundance of SaAqp1b was higher in rectum. In duodenum and hindgut, SaAqp1a localized at the apical brush border and lateral membrane of columnar enterocytes, whereas SaAqp1b was detected occasionally and at very low levels at the apical membrane. In the rectum, however, SaAqp1a was mainly accumulated in the cytoplasm of a subpopulation of enterocytes spreaded in groups over the surface of the epithelia including the intervillus pockets, while SaAqp1b was detected exclusively at the apical brush border of all rectal enterocytes. Freshwater-acclimation reduced the synthesis of SaAqp1a protein in all intestinal segments, but it only reduced SaAqp1b abundance in the rectum. These results show for the first time in teleosts a differential distribution and regulation of two functional AQP1 homologs in the intestinal epithelium, which suggest that they may play specialized functions during water movement across the intestine.

Gilthead seabream; SaAqp1a; SaAqp1b; functional expression; salinity; gastrointestinal tract

INTRODUCTION

Osmoregulation in teleost fish is achieved by integrating ion and water transport mechanisms in the gills, kidney, gastrointestinal tract and urinary bladder (5, 9). To compensate for osmotic water loss and dehydration, marine teleosts drink relatively large amounts of seawater (SW), absorb most of this water and monovalent ions across the intestine, secrete excess of ions from gill chloride cells, and excrete a modest amount of near-isoosmotic urine (17). Ingested SW is mainly desalted in the oesophagus, which absorbs Na^+ and Cl^- through both passive and active transport pathways, and thereafter along the entire length of the intestine, by active transport of monovalent ions into the blood (17, 18, 36). The subsequent water absorption takes place in the intestine by osmotic mechanisms following active absorption of monovalent ions (17, 44, 45). Thus, in euryhaline fish, intestinal water absorption is critical for water balance, especially when fish acclimate to SW during their life cycle (4, 9, 17). However, it is yet unclear whether water in the fish intestine is absorbed through transcellular or paracellular routes and which water specific carrier proteins may play a direct role in water movement.

The molecular water channels or aquaporins (AQPs) are members of the major intrinsic proteins (MIP) family of integral membrane proteins that exists in virtually every living organism (1). These proteins are structurally related and function as water channels involved in fluid transport within various organs, although some of them are also permeable to small solutes, such as glycerol and urea (aquaglyceroporins). The AQPs consist of six transmembrane domains connected by five loops (A-E) and have their N and C terminus located intracellularly. One molecule consist of two repeats, which are 180º mirror images

of each other, and each repeat contains the highly-conserved asparagine-proline-alanine (NPA) motif (in loops B and E), which is the hallmark of the MIP family of proteins to which AQPs belong. The folding of loops B and E is important for the formation of the water pore as it has been corroborated by the determination of the three-dimensional structure of AQP0, AQP1 and AQP9 (16).

The potential role of AQPs in water transport across the gastrointestinal tract of teleosts has been recently investigated. Although few complementary DNAs (cDNAs) encoding fish AQPs have been isolated so far, a number of studies have demonstrated the presence of mRNA and/or protein of aquaporin-1 (Aqp1), aquaporin-3 (Aqp3), and of two aquaglyceroporins, named AQPe and sbAQP, in the oesophagus, stomach and/or intestine of several teleosts (4, 10-12, 15, 21, 29, 36-38, 43, 50). In catadromous teleosts, such as the European eel (*Anguilla anguilla*) and Japanese eel (*A. japonica*), Aqp1 is found at the apical membrane of intestinal columnar enterocytes, and transition from freshwater (FW) into SW, as well as treatment of fish with the "SW-adapting" hormone cortisol, upregulates Aqp1 synthesis in epithelial cells of all intestinal segments (4, 36). In agreement with this, FW acclimation of the marine teleost sea bass (*Dicentrarchus labrax*) downregulates *aqp1* mRNA expression in intestinal epithelial cells (15). These observations thus suggest that fish Aqp1 may play a pivotal role in the control of intestinal water absorption in teleosts under SW conditions.

The gilthead seabream (*Sparus aurata*) is a marine teleost that inhabits coastal waters, capable of adapting to considerable changes in environmental salinity (31). Previous studies with this species showed that a decrease in salinity activates the release of the “FW-adapting” hormone prolactin, growth hormone and melatonin (25, 32, 34), induces changes

in gill Na^+,K^+-ATPase and thyroid hormone-metabolizing enzymes and thyroid plasma levels (24, 28), and leads to transitory blood hypomineralization (30). Additionally, prolactin and cortisol control the Na^+,K^+-ATPase activity and blood osmolality in fish maintained in brackish water, thus improving its hypoosmoregulatory capacity (27, 33, 35). However, in this species, as well as in other marine teleosts, there is no information on the cellular localization of AQPs in the gastrointestinal tract and the effects of changes in salinity.

In the seabream, we have recently isolated the cDNAs encoding two AQP homologs of mammalian AQP1, called *S. aurata* Aqp1 (SaAqp1) and *S. aurata* Aqp1 of the ovary (SaAqp1o). The corresponding genes have been found in other teleosts (7, 47) and they seem to be evolved from a teleost-specific local duplication of an ancestral *AQP1* gene during evolution, and accordingly they should be named Aqp1a and Aqp1b, respectively (7, 13, 47). In the seabream, both orthologs show a completely distinct pattern of expression, while SaAqp1a is present in most organs including the intestine, gills and kidney, SaAqp1b is found predominantly in the oocyte, where it is involved in water uptake during meiotic maturation (13, 14, 47). In the present work, we show that SaAqp1a and SaAqp1b are both functional water channels when expressed in *Xenopus laevis* oocytes, and that SaAqp1b is in fact synthesized by intestinal epithelial cells, as is SaAqp1a, in addition to the oocyte. However, the cellular localization of both AQPs along the entire length of the intestine, as well as the changes in protein abundance under different salinity conditions (SW and FW), appeared to be different.

MATERIALS AND METHODS

Fish

Gilthead sea bream juveniles (100-300 g in body weight), reared in captivity at the Center of Aquaculture IRTA and acclimated in SW, were divided into two groups (n = 20) and placed in 1,500-litre tanks. One tank was maintained in SW (30‰ salinity), while the other was in FW (1-2‰ salinity). Both SW- and FW-acclimated fish were starved and maintained under natural conditions of photoperiod (12 h light, 12 h dark) and temperature (20ºC) for 10 days before a subsample of fish (n = 6) was sacrificed. Fish were sedated with 100 ppm phenoxyethanol and immediately killed by decapitation. Pieces (approximately 100 mg) of the duodenum, hindgut and rectum were frozen in liquid nitrogen and stored at -80ºC, or fixed for immunohistochemistry. All procedures for the sacrifice of fish were approved by the Ethics and Animal Experimentation Committee from IRTA (Spain).

Antibodies

Commercially prepared (Cambridge Research Biochemicals, U. K.) specific antisera against SaAqp1a was raised in rabbits by immunization with a synthetic peptide corresponding to the C termini of the corresponding deduced amino acid sequence, GDYDVNGGNDATAVEMTSK (GenBank accession number AY626939). The antisera was affinity-purified on thiopropyl sepharose 6B coupled to the synthetic peptide. The specificity of the resulting fraction was tested by ELISA, and by immunofluorescence microscopy and Western blot of *X. laevis* oocytes expressing SaAqp1a. Production of antisera against a synthetic peptide corresponding to the C termini of SaAqp1b, PREGNSSPGPSQGPSQWPKH (GenBank accession number AY626938), has been previously described (13).

Functional Expression in X. laevis Oocytes

Transcription of pT7Ts-SaAqp1a and pT7Ts-SaAqp1b constructs, and isolation, defolliculation and injection of *X. laevis* oocytes were done as described previously (13). The osmotic water permeability (P_f) was measured from the time course of osmotic oocyte swelling in a standard assay. Oocytes were transferred from 200 mOsm modified Barth's medium (MBS) to 20 mOsm MBS medium at room temperature, and the swelling of the oocytes was followed under a stereomicroscope using serial images at 2-s intervals during the first 20 s period. The P_f values were calculated as described (43). To examine the effect of mercury on the P_f, oocytes injected with 1 ng SaAqp1a cRNA or 2 ng SaAqp1b cRNA were incubated in MBS containing 0.7 mM $HgCl_2$ for 15 min before the swelling assay, which was also performed in the presence of $HgCl_2$. To determine if the mercurial effect was reversible, the same oocytes were rinsed 3 times in MBS, incubated with 5 mM β-mercaptoethanol for 15 min, and subjected to the swelling assays 2 h later. The apparent glycerol permeability coefficient (P'_{gly}) of water-, SaAqp1a- and SaAqp1b-injected oocytes was determined from oocyte swelling as described (43).

Real-Time Quantitative RT-PCR

The abundance of seabream *aqp1a* and *aqp1b* transcripts in the different regions of the intestine was determined by by real-time quantitative RT-PCR (qPCR). Total RNA was extracted from samples of duodenum, hindgut and rectum (n = 3 fish) with the RNeasy Mini kit (Qiagen). After DNAse treatment with DNAse I using the RNase-Free DNase kit (Qiagen), 1 µg of total RNA from each intestinal region (in triplicate) from each fish was reverse-transcribed into cDNA using 10 IU MMLuV-RT enzyme (Roche), 0.5 µM oligo-(dT)12-18 (Invitrogen) and 1 mM dNTPs, in a 20-µl volume reaction, for 1.5 h at 50ºC. Real-time qPCR amplifications were performed in a final volume of 20 µl with 10 µl SYBR® Green qPCR master mix (Applied Biosystems), 2 µl diluted

(1/10) cDNA, and 0.5 μM of each forward and reverse primer. For *aqp1a*, the forward and reverse primers were 5'-GGCTCTCACGTACGATTTCC-3' and 5'-TCTGTGTGGGACTATTTTGACG-3', respectively, which amplified a fragment of 153 bp. For *aqp1b*, the forward oligonucleotide primer was 5'- GCGACGGAGTGATGTCAAAGG-3', and the reverse primer was 5'-AGATAAGAGCCGCCGCTATGC-3', which amplified a fragment of 203 bp. Both primer pairs were located flanking the last intron to exclude genomic contamination. The sequences were amplified in duplicate for each cDNA on 384-well plates using the ABI PRISM 7900HT sequence detection system (Applied Biosystems). The amplification protocol was as follows: and initial denaturation and activation step at 50ºC for 2 min, and 95ºC for 10 min, followed by 40 cycles of 95ºC for 15 sec and 63ºC for 1min. After the amplification phase, a temperature-determinating dissociation step was carried out at 95ºC for 15 sec, 60ºC for 15 sec and 95ºC for 15 sec. For normalization of cDNA loading, all samples were run in parallel using 18S ribosomal protein (*18S*) as reference gene (GenBank accession number EF126042). Forward primer was 5'-GAATTGACGGAAGGGCACCACCAG-3', and reverse primer was 5'-ACTAAGAACGGCCATGCACCACCAC-3', which amplified a 148-bp fragment. To estimate efficiencies, a standard curve was generated for each primer pair from 10-fold serial dilutions (from 100 to 0.01 ng) of a pool of first-stranded cDNA template from all samples. Standard curves represented the cycle threshold (Ct) value as a function of the logarithm of the number of copies generated, defined arbitrarily as 1 copy for the most diluted standard. All calibration curves exhibited correlation coefficients higher than 0.99, and the corresponding real-time PCR efficiencies were above 99%.

Western Blotting

Total membranes were isolated from water-, SaAqp1a- and SaAqp1b-injected *X. laevis* oocytes (10 oocytes), as well as from pieces (approximately 100 mg) of duodenum, hindgut and

rectum of seabream maintained in SW and FW. Tissues were homogenized in HbA buffer, containing 20 mM Tris pH 7.4, 5 mM $MgCl_2$, 5 mM NaH_2PO_4, 1 mM EDTA, 80 mM sucrose, and cocktail of protease inhibitors (Mini EDTA-free; Roche), and centrifuged for 2 times 5 min each at 200 x g at 4ºC (23). Total membranes were isolated by a final 20 min centrifugation step at 13,000g at 4ºC, and resuspended in 1% NP-40, 1 mM $CaCl_2$, 150 mM NaCl, 10 mM Tris pH 7.4, and protease inhibitors. An aliquot of the homogenate was kept for determination of protein concentration using the Bio-Rad Protein assay kit, and the rest was mixed with 2 x Laemmli sample buffer (26) and frozen at -80°C. For immunoblotting, a volume of Laemmli-mixed homogenate corresponding to 0.2 oocyte equivalents or 20 μg of total protein was subjected to electrophoresis on 12% SDS-PAGE. Proteins were blotted onto PVDF membranes (Bio-Rad Laboratories) in high glycine transfer buffer (190 mM glycine, 250 mM Tris, pH 8.6, 20% methanol). Membranes were blocked for 1 h at room temperature in 5% non-fat dried milk in Tris-buffered saline 0.1% Tween (TBST), and incubated overnight (1:300) with SaAqp1a or SaAqp1b rabbit antisera. Bound antibodies were detected with goat anti-rabbit IgG antibodies (1:8,000) coupled to horseradish peroxidase using enhanced chemiluminescence (ECL detection system; Amersham). Control membranes were incubated with the antisera preadsorbed with a 30-fold molar excess of the corresponding immunizing peptides. For quantitation of SaAqp1a and SaAqp1b protein abundance, three separate membranes (for the duodenum, hindgut and rectum, respectively), each containing samples of both SW- and FW-acclimated fish, were incubated with each antisera in duplicate. The signal intensity of SaAqp1a and SaAqp1b reactive bands was optimized for each intestinal segment by exposing each membrane to X-ray films for different times. The density of the bands was measured using the Quantity-One software (Bio-Rad Laboratories).

Immunofluorescence Light Microscopy

X. laevis oocytes injected with water and with SaAqp1a or SaAqp1b cRNAs, and pieces of seabream duodenum, hindgut and rectum, were fixed in Bouin's without acetic acid (for SaAqp1a detection) or 4% paraformaldehyde in PBS (for SaAqp1b detection), for 4-6 h at room temperature, and subsequently dehydrated and embedded in Paraplast (Sigma). Sections of approximately 6 μm were blocked with 5% goat serum in PBST (0.1% BSA, 0.01% Tween-20 in PBS), and incubated with SaAqp1a or SaAqp1b antisera (1:100) in PBST with 1% goat serum overnight at 4°C. Sections of duodenum and hindgut processed for SaAqp1b were permeabilized with 1% SDS in PBS for 10 min at room temperature before the blocking step. After four washes with PBS, 5 min each, the sections were incubated with FITC anti-rabbit secondary antibodies (1:300 in PBS) for 1 h, washed three times with PBS and mounted with Vectashield (Vector Labs). Control sections were incubated with the antisera previously incubated with the corresponding synthetic peptides as described above, or with the preimmune sera (not shown). In both cases, no positive staining was observed, with only nonspecific autofluorescence in red blood cells (not shown). Immunofluorescence was observed and documented with a Leica TCS SP confocal microscope.

Data Analysis

The data on *aqp1a* and *aqp1b* mRNA levels and P_f of oocytes injected with water or with SaAqp1a or SaAqp1b cRNAs, in the presence or absence of $HgCl_2$ and β-mercaptoethanol, were analyzed by one-way ANOVA. The data on SaAqp1a and SaAqp1b protein abundance in the duodenum, hindgut and rectum were analyzed with the Student's *t* test. The level of significance was set at $P \leq 0.05$.

RESULTS

The SaAqp1a and SaAqp1b are Functional, Water-Selective AQPs

The deduced amino acid sequence of SaAqp1a and SaAqp1b cDNAs are most similar to mammalian AQP1, SaAqp1a being slightly more similar to AQP1 (57-59% identity) than SaAqp1b (45-54% identity) (13). However, seabream SaAqp1a and SaAqp1b are only 60% identical, similarly as it occurs between Aqp1 and Aqp1dup from European eel (69% identity; Ref. 37), which are the eel Aqp1a and Aqp1b orthologs, respectively (7, 15, 47). The comparison of the primary structure of AQP1-like polypeptides between human, seabream and European eel indicated that teleost AQP1-related sequences show the six potential transmembrane (TM) domains, the two NPA motifs, and the residues of the pore-forming region (Phe^{56}, His^{180} and Arg^{195}; human AQP1 numbering) in TM2, TM5 and loop E that are conserved in water-selective AQPs (46) (Fig. 1, *A* and *B*). All the amino acid sequences also showed the Cys residue before the second NPA motif (Cys^{178} for SaAqp1a and SaAqp1b), which is the potential responsible site for the inhibition of water permeability by mercurial compounds (42).

The relatively high conserved amino acid sequence of TM2 and TM5, as well as of loops B and E, of SaAqp1a and SaAqp1b with respect to the corresponding regions of human AQP1 (Fig. 1*B*) suggested that both fish paralogs might encode functional water channels. To confirm this, *X. laevis* oocytes injected with cRNAs encoding SaAqp1a or SaAqp1b were compared with oocytes injected with 50 nl of water. Immunofluorescence microscopy confirmed that SaAqp1a and SaAqp1b cRNAs were translated into their respective polypeptides which were translocated into the oocyte plasma membrane,

229 although SaAqp1b appeared to be partially retained in the cytoplasm (Fig. 1, *C* and *D*).
230 Coefficients of P_f were determined from rates of oocyte swelling after transfer to
231 hypoosmotic MBS solution (Fig. 1*E*). Water-injected oocytes exhibited low water
232 permeability, whereas the P_f of oocytes injected with 1 ng SaAqp1a cRNA increased by
233 approximately 50 fold, and those injected with 2 ng SaAqp1b cRNA increased by 18 fold.
234 The presence of 0.7 mM $HgCl_2$ reduced the P_f of both SaAqp1a- and SaAqp1b-injected
235 oocytes by approximately 87% and 82%, respectively. For SaAqp1a oocytes, the inhibition
236 was completely recovered by incubation of oocytes with 5 mM β-mercaptoethanol, whereas
237 for SaAqp1b oocytes the treatment with β-mercaptoethanol partially reversed the mercurial
238 inhibition (42% recovery). The P'_{gly} of oocytes expressing SaAqp1a or SaAqp1b was not
239 different from that of control oocytes indicating that SaAqp1a or SaAqp1b were not
240 permeable to glycerol (data not shown). These data thus indicated that both SaAqp1a and
241 SaAqp1b were functional water channels whose permeability properties resembled those of
242 mammalian AQP1 (41).
243
244 *Differential mRNA Expression and Protein Abundance of SaAqp1a and SaAqp1b Along the*
245 *Intestine*
246 To investigate the presence of SaAqp1a and SaAqp1b in the different portions of the
247 seabream intestine, we first determined the abundance of *aqp1a* and *aqp1b* mRNAs by
248 qPCR (Fig. 2*A*). The results of these experiments indicated that *aqp1a* transcripts were
249 equally abundant in duodenum and hindgut but they accumulated significantly less ($P <$
250 0.01) in rectum. On the contrary, *aqp1b* mRNAs in duodenum and hindgut were similar

but significantly lower ($P < 0.01$) than those in rectum, thus showing an opposite distribution than that of *aqp1a*.

Western blotting analysis on protein extracts from the different regions of the intestine was subsequently carried out using SaAqp1a and SaAqp1b specific antisera to detect the presence of the corresponding polypeptides (Fig. 2*B*). Immunoblotting on total membrane protein extracts from *X. laevis* oocytes injected with water or cRNAs encoding SaAqp1a or SaAqp1b, using the SaAqp1a antisera, showed a single protein band with a molecular mass of approximately 26 kDa in extracts from oocytes injected with SaAqp1a, thus being consistent with the molecular mass of SaAqp1a (26.1 kDa) calculated from the deduced amino acid sequence of its cDNA (Fig. 2*B*, *left panel*, *lane 2*). This band was absent in water- and SaAqp1b-injected oocytes (Fig. 2*B*, *left panel*, *lanes 1* and *3*). In the extracts from the three intestinal segments, the SaAqp1a-reactive band was also present but its intensity was higher in the duodenum and hindgut than in the rectum (Fig. 2*B*, *left panel*, *lanes D, H* and *R*). In protein extracts from intestine, but not in those from *X. laevis* oocytes, two additional weaker bands of approximately 31 and 39 kDa were detected. The 31-kDa band might correspond to a glycosylated form since SaAqp1a shows a glycosylation motif in extracellular loop E (Asn^{194}; Fig. 1*B*), whereas the 39-kDa band could be a dimer (22, 49). Control blots incubated with the SaAqp1a antisera preadsorbed with large amounts of the immunizing peptide were negative (Fig. 2*B*, right panel), indicating the specificity of the reaction.

Immunoblotting with the same protein extracts and the SaAqp1b antisera identified two very close immunoreactive bands with a molecular mass of approximately 27 and 29 kDa in oocytes injected with SaAqp1b, in agreement with the calculated molecular mass

(27.2 kDa) of the SaAqp1b amino acid sequence deduced from its cDNA (Fig. 2*C*, *left panel, lane 3*). Lanes from the same blot corresponding to water- and SaAqp1a-injected oocytes were negative (Fig. 2*C*, *left panel, lanes 1* and *2*), thus confirming the absence of cross-reaction between the SaAqp1a and SaAqp1b antisera. In total membrane extracts from seabream duodenum and hindgut, a single SaAqp1b immunoreactive band of approximately 28 kDa was observed, while in the rectum two prominent bands of 27 and 29 kDa, apparently the same that were observed in oocyte extracts, were detected (Fig. 2*C*, *left panel, lanes D, H* and *R*). The intensity of the single bands in the duodenum and hindgut was lower than that of the double bands present in the rectum. Control blots incubated with preadsorbed SaAqp1b antisera did not show any protein band (Fig. 2*C*, right panel).

Cellular Localization of SaAqp1a and SaAqp1b in the Intestine

The cellular distribution of both SaAqp1a and SaAqp1b in the seabream intestine was characterized by immunofluorescence light microscopy. In the duodenum and hindgut, an intense SaAqp1a immunoreactivity was detected in the apical brush border of epithelial cells, suggesting that SaAqp1a was localized on or very close to the apical microvilli (Fig. 3, *A*-*C*). The lateral membrane of the columnar epithelial cells also showed SaAqp1a immunofluorescence, although the intensity was apparently lower than in the brush border. Specific SaAqp1a immunostaining was also detected in endothelial cells of blood vessels within the submucosa and muscular layers (Fig. 3*C*). The goblet intestinal cells, however, were negative for SaAqp1a staining (Fig. 3, *A* and *C*). The SaAqp1b immunoreactivity in the duodenum and hindgut was detected specifically in the brush border of the epithelial cells (Fig. 4, *A* and *B*). However, there was a considerable variability in the intensity of the

297 SaAqp1b immunoreaction in these regions, the signal being in general much weaker than
298 that observed by using the SaAqp1a antisera, even after a detergent permeabilization of the
299 histological sections before incubation with the primary antibody. Unlike for SaAqp1a,
300 vascular endothelia and red blood cells were apparently devoid of SaAqp1b (Fig. 4, *A* and
301 *B*).

302 In the rectum, a different pattern of SaAqp1a localization with respect to that found in
303 the duodenum and hindgut was observed. In this region, strong SaAqp1a staining was
304 detected almost exclusively in the intracellular subapical compartment of some specific
305 epithelial cells randomly distributed within the epithelia as well as located at the base of the
306 intervillus pockets (Fig. 5, *A* and *C*), which are possibly analogous to crypts of Lieberkühn
307 from mammals (8). These cells had a more rounded nucleus, with a well visible nucleolus,
308 and a lower amount of eosinophilic (i.e., basic) granules in the subapical compartment than
309 columnar enterocytes (Fig. 5*D*). A faint SaAqp1a staining was however also observed in
310 the perinuclear compartment, as well as in the apical brush border and lateral membrane, of
311 enterocytes containing many eosinophilic granules outside of the intestinal folds (Fig. 5*B*).
312 By contrast, the SaAqp1b antisera intensively stained the brush border of both types of
313 rectal enterocytes, indicating a restricted localization of SaAqp1b in the apical membrane
314 (Fig. 6, *A*-*C*). As it occurred in the duodenum and hindgut, the endothelial cells of blood
315 vessels from the rectum were also strongly stained with the SaAqp1a (Fig. 5*A*) antisera but
316 not with the SaAqp1b antisera, and there were no apparent differences in SaAqp1a
317 immunoreactivity in these areas between rectum, duodenum and hindgut. The
318 immunohistochemistry results were thus consistent with previous qPCR and Western
319 blotting analysis indicating that the rectum showed the lowest abundance of SaAqp1a and

320 the highest abundance of SaAqp1b. This may be caused by the accumulation of SaAqp1a
321 mainly in the cytoplasm of a subpopulation of rectal enterocytes, while SaAqp1b was
322 highly expressed at the brush border of all enterocytes of the rectum.
323
324 *Effect of FW Acclimation on SaAqp1a and SaAqp1b Protein Abundance in the Intestine*
325 Western blotting analysis was performed employing the same antisera as before and
326 purified cell membrane fractions from the intestine of fish maintained in SW and of fish
327 acclimated to FW for 10 days (Figs. 7*A* and 8*A*). Quantification of immunoblots
328 determined that FW acclimation of seabream resulted in a significant decrease in SaAqp1a
329 expression throughout the whole intestine ($P < 0.05$), this decrease being especially marked
330 in the rectum (approximately by 80%) (Fig. 7*B*). However, FW acclimation only reduced
331 significantly ($P < 0.05$) SaAqp1b protein abundance in the rectum (approximately by 50%),
332 while in duodenum and hindgut the levels of this protein remained unchanged (Fig. 8*B*).
333
334 **DISCUSSION**
335
336 It is well established that AQP water channels are a family of membrane proteins that
337 facilitate water movement across cell membranes in plants and animals (1). Thus far, at
338 least 13 distinct AQPs have been discovered in mammals, from which some are water-
339 selective (AQP0, -1, -2, -4, -5, -6, and -8), some are aquaglyceroporins (AQP3, -7, -9 and -
340 10), and two (AQP11 and -12) belong to a closely related subfamily which permeability
341 properties have not been yet conclusively characterized (1, 20, 51). Recent efforts to clone
342 and characterize teleost AQPs indicate the expression of two different AQP1 orthologs in

343 this group of vertebrates (13, 37), unlike in mammals, as well as a number of different
344 aqualyceroporin paralogs (4, 10-12, 15, 36, 37, 43, 50). However, the permeability
345 properties of most fish AQPs and aquaglyceroporins have not been yet reported, which
346 makes difficult to understand their physiological roles. Based on phylogenetic and
347 genomic analysis, we have recently proposed to name the two fish AQP1 orthologs as
348 Aqp1a and Aqp1b, the latter group including the SaAqp1o and the European eel Aqp1dup
349 (7, 47). In the present work, it is shown that SaAqp1a and SaAqp1b are both water-
350 selective channels which permeability properties are similar to those of human AQP1, and
351 thus they can be classified as true AQP1 paralogs.
352 The gilthead seabream has a short intestine that is largely divided into two regions,
353 the anterior intestine or duodenum and the posterior intestine or hindgut (6). After the
354 posterior intestine, there is a narrowing corresponding to a valve, marking the pass to the
355 rectum. The epithelia of the duodenum and hindgut is typically folded forming the villi that
356 protrude into the lumen and the intervillus pockets, and it consists of columnar cells, the
357 enterocytes, intercalated with the mucus-secreting goblet cells, which increase in number
358 towards the lower part of the intestine (6). The rectal epithelia is also folded and is
359 characterized by enterocytes containing many vacuoles filled with eosinophilic granules.
360 This study showed that SaAqp1a was expressed in epithelial enterocytes from all intestinal
361 segments of SW-acclimated seabream, with the duodenum and hindgut showing the highest
362 mRNA and protein levels. The presence of Aqp1a in fish intestinal enterocytes agrees with
363 previous reports in SW-acclimated eels and sea bass, where the Aqp1a ortholog is mainly
364 expressed by columnar enterocytes of the posterior intestine, whereas Aqp3 is found in
365 intra-epithelial “macrophage-like” and goblet cells of the rectal epithelium (4, 15, 29, 36).

These findings, however, contrast with the situation in mammals, where AQP1 has not been reported in normal epithelial cells lining the gastrointestinal system, but exclusively in microvascular endothelia (30, 39). The localization of AQP1 in gastrointestinal epithelial cells has only been demonstrated in tumors of the colon, where it seems to contribute to tumor angiogenesis and the formation of high fluid pressures and high vascular permeability of tumor microvessels (40). The differences in the intestinal localization of AQP1 between fish and mammals are probably related to the fact that the gastrointestinal tract of teleosts plays an important osmoregulatory role (17).

Water absorption across the marine teleost intestine is tightly linked to the absorption of Na^+ into the enterocytes fueled by the basolateral Na^+, K^+-ATPase, which provides the energy necessary for the active transport of K^+ and Cl^- from the intestinal lumen by apical co-transporters (17). The highest abundance of SaAqp1a protein in the duodenum and hindgut, mostly located at the apical plasma membrane of enterocytes, suggests that in seabream these intestinal regions may play a major role in SaAqp1a-mediated water absorption following the uptake of ions. This conclusion would be consistent with earlier reports which indicate that the highest levels of water flux within the teleost intestine occur in the mid-region, followed in descending order by the posterior and anterior intestine, and finally the rectum (2, 3). The seabream aquaglyceroporin sbAQP, however, is not likely to be involved in water transport across the intestinal epithelia, since its mRNA is found only in cells scattered in the lamina propria and at the interface of the circular and longitudinal muscle layer of the hindgut (43). In SW-acclimated silver eels, as in seabream, the rectal epithelium shows low Aqp1a expression, whereas the posterior/rectal intestinal segment exhibits the highest amount of Aqp1a mRNA and protein (36). In this intestinal segment of

389 the eel, Aqp1a localizes preferentially in the apical membrane of epithelial cells which is
390 consistent with the highest water absorption rates found in the eel posterior intestine (4, 36).
391 In this species, expression of AQPe, a putative aquaglyceroporin, is found in all intestinal
392 segments but its cellular localization is unknown (36).
393 Unlike in duodenum and hindgut, SaAqp1a immunoreactive peptides in rectum
394 mainly accumulated in the cytoplasm, surrounding the nucleus, of groups of enterocytes
395 spreaded within the epithelia and located at the base of the intervillus pockets. In the rest of
396 enterocytes, much weaker SaAqp1a immunoreaction was found within the perinuclear
397 compartment and in the apical brush border and lateral plasma membrane. In fish,
398 intestinal stem cells, responsible for the renewal of the gut epithelium, are confined to the
399 base of the intervillus pockets, which also contains stem cell dividing offspring-committed
400 progenitors undergoing divisions prior to terminal differentiation (8). Thus, the cells
401 located at the base of the rectal pockets showing SaAqp1a cytoplasmic localization could
402 correspond to intestinal progenitors committed to differentiate into enterocytes. The
403 localization of Aqp1a in these cells has not been reported in any other fish species, and
404 therefore the precise nature of these cells awaits further investigation.
405 In the European eel, mRNA encoding Aqp1dup (i.e., the eel Aqp1b paralog) is
406 accumulated in the oesophagus and kidney but it has not been found in the intestine of
407 either FW- or SW-adapted eels by using semi-quantitative Northern blot (37, 38). In SW-
408 acclimated seabream, we have found that *aqp1b* mRNA is expressed in the different
409 segments of the intestine, although the rectum showed the highest levels. Such a
410 discrepancy with the data reported in eel is possibly caused by the lower expression level of
411 *aqp1b* mRNA in the intestine of SW-adapted eels when compared with that in oesophagus

412 or kidney (47), which may only be detected by qPCR. In the seabream, according with the
413 mRNA levels, the highest abundance of SaAqp1b protein was observed in rectum, where
414 two bands possibly corresponding to phosphorylated and non-phosphorylated forms (47)
415 were detected, although some variability between fish was also observed. However,
416 Western blotting analysis of membrane fractions from duodenum and hindgut revealed the
417 presence of one single SaAqp1b reactive band migrating approximately between the two
418 bands present in membrane fractions from SaAqp1b-injected *X. laevis* oocytes, expressing
419 functional SaAqp1b, and rectum. Interestingly, SaAqp1b was poorly detected by
420 immunofluorescence microscopy in duodenum and hindgut. Recent studies using
421 heterologous expression in *X. laevis* oocytes have shown that expression of SaAqp1b
422 bearing a mutated C terminus that induces its retention in the endoplasmic reticulum (ER)
423 and partial degradation results in an identical electrophoretic profile (47). Thus, the
424 unusual electrophoretic profile of SaAqp1b extracted from the duodenum and hindgut,
425 together with its poor immunocytochemical detection, suggests that the protein detected by
426 Western blot in these intestinal segments may be retained in the ER and thus not functional.
427 In the rectum, SaAqp1b immunostaining was restricted exclusively to the apical
428 brush border of the enterocytes, and thus it showed a distinct distribution than SaAqp1a in
429 this intestinal region. Interestingly, FW adaptation produced a reduction in SaAqp1b
430 protein abundance in the rectum (by approximately 50%) but not in the duodenum or
431 hindgut. The eel *aqp1b* mRNA expression in oesophagus is upregulated after cortisol
432 treatment, while in the kidney both *aqp1a* and *aqp1b* transcripts are downregulated after
433 cortisol infusion or SW acclimation (37). These findings thus suggest that although teleost
434 Aqp1b seems to be an specialised AQP involved in water uptake by the oocyte during

steroid-induced meiotic maturation (13, 14), it may also play other osmoregulatory roles in somatic tissues, such as water absorption across the rectal epithelium. Based on the relative amount of SaAqp1a and SaAqp1b peptides along the entire length of the seabream intestine, it is possible to speculate that in the rectum SaAqp1a may have a limited role in water absorption leaving to SaAqp1b the bulk of water transport. However, the synthesis of SaAqp1b, although may be not functional, also occurred in the duodenum and hindgut, and was apparently not altered by changes in salinity. Future studies will be necessary to elucidate the mechanisms involved in SaAqp1b protein synthesis and sorting into the plasma membrane in intestinal enterocytes, as well as the physiological significance of SaAqp1a and SaAqp1b co-expression in rectal enterocytes, which remains intriguing.

The immunocytochemical detection of SaAqp1a and SaAqp1b in the epithelial intestine of seabream, as well as of Aqp1a in other teleosts (4, 36), may favour the hypothesis of a transcellular pathway during the active water transport mechanism in the intestine under high salinity conditions. Although the presence of an AQP-mediated mechanism in the fish intestine has not been yet functionally demonstrated, it may be supported by the observation that SW conditions induce *aqp1a* and *aqp1b* mRNA expression and/or protein synthesis in the intestinal epithelium (4, 15, 36, present work). Moreover, it has been shown that injection of cortisol into FW eels upregulates the expression of Aqp1a throughout the intestine and elevates intestinal permeability with commensurate increases in the net absorption of monovalent ions and water (19, 36, 48). The presence of Aqp1a in vascular endothelia within the submucosa and muscular layers of the intestine (4, 36, present work) may provide an additional exit pathway for water absorbed by the intestinal epithelia to flow into the blood circulation. However, the present

458 and previous works have failed to conclusively demonstrate the presence of AQPs in the
459 basal membrane of teleost enterocytes which might be required to transport water across
460 the intestinal epithelia. Therefore, the investigation of the presence of additional AQPs in
461 the fish intestine is necessary to gain a more complete understanding of the anatomical
462 localization and molecular identity of AQPs in the teleost gastrointestinal tract as well as of
463 their functions.
464
465 *Perspectives and Significance*
466 This study is the first to demonstrate the differential expression, localization and
467 regulation during FW acclimation of two teleost-specific AQP1 homologs, Aqp1a and
468 Aqp1b, in the enterocytes along the intestine of an euryhaline teleost. Although direct
469 experimental evidence is still lacking, these findings provide further support for the role of
470 AQP1-like channels in mediating water absorption across the intestine of SW-acclimated
471 fish. However, based on the relative abundance of mRNA and protein along the intestine,
472 in addition to their specific cellular localization, it is intriguing to speculate that SaAqp1a
473 and SaAqp1b may play specialized roles in duodenum/hindgut and rectum, respectively, for
474 water absorption. The present and previous studies thus suggest that teleost Aqp1b has
475 possibly been neofunctionalized in some osmoregulatory cells (i.e., oocytes and rectal
476 enterocytes) following gene duplication. Future studies will be necessary to elucidate the
477 physiological significance of this evolutionary process within the teleost lineage, as well as
478 the associated isoform-specific regulatory mechanisms, which will help understand the
479 osmoregulatory adaptations underlying the vertebrate radiation.
480 **ACKNOWLEDGEMENTS**

This work was supported by Grants from the Spanish Ministry of Education and Science (AGL2001-0364/ACU and AGL2004-00316) and the European Commission (Q5RS-2002-00784-CRYOCYTE), and by the Reference Center in Aquaculture (Generalitat de Catalunya, Spain) to J. Cerdà. Participation of M. Fabra and D. Raldúa was financed by a fellowship from the Catalan Government (DURSI, Spain), and by a "Ramón y Cajal" contract (MEC), respectively.

Present addresses: D. Raldúa, Laboratory of Environmental Toxicology, Universidad Politécnica de Catalunya, Ctra. Nac. 150, km. 14.5 -Zona IPCT, TR-23 -Campus Terrassa, 08220 Terrassa, Spain; M. Fabra, Department of Genetic Medicine and Development, 8242 CMU, 1 rue Michel Servet, University of Geneva Medical School, 1211 Geneva 4, Switzerland.

REFERENCES

1. **Agre P, King SL, Yasui M, Guggino WB, Ottersen OP, Fujiyoshi Y, Engel A, and Nielsen S.** Aquaporin water channels – from atomic structure to clinical medicine. *J Physiol* 542: 3-16, 2002.
2. **Ando M.** Chloride-dependent sodium and water transport in the seawater eel intestine. *J Comp Physiol* 138B: 87-91, 1980.
3. **Ando M and Kobayashi M.** Effects of stripping of the outer layers of the eel intestine on salt and water transport. Comp Physiol Biochem 61A: 497-501, 1978.
4. **Aoki M, Kaneko T, Katoh F, Hasegawa S, Tsutsui N, and Aida, K.** Intestinal water absorption through aquaporin 1 expressed in the apical membrane of mucosal epithelial cells in seawater-adapted Japanese eel. *J Exp Biol* 206: 3495-3505, 2003.
5. **Bentley PJ.** *Endocrines and Osmoregulation*. *Zoophysiology* Vol. 39. Berlin: Springer, 2002.

6. **Cataldi E, Cataudella S, Monaco G, Rossi A, and Tancioni L.** A study of the histology and morphology of the digestive tract of the sea-bream, *Sparus aurata*. *J Fish Biol* 30: 135-145, 1987.

7. **Cerdà J, Fabra M, and Raldúa D.** Physiological and molecular basis of fish oocyte hydration. In: *The Fish Oocyte: From Basic Studies to Biotechnological Applications*, edited by Babin P, Cerdà J and Lubzens E. The Netherlands: Springer, 2007, p. 349-396.

8. **Crosnier C, Vargesson N, Gschmissner S, Ariza-McNaughton L, Morrison A, and Lewis J.** Delta-Notch signalling controls commitment to a secretory fate in zebrafish intestine. *Development* 132: 1093-1104, 2005.

9. **Cutler C and Cramb G.** Water transport and aquaporin expression in fish. In: *Molecular Biology and Physiology of Water and Solute Transport*, edited by Hohmann S, Nielsen S and Agre P. London: Kluwer Academic Press, 2000, p. 431-441.

10. **Cutler CP and Cramb G.** Branchial expression of an aquaporin 3 (AQP-3) homologue is downregulated in the European eel *Anguilla anguilla* following seawater acclimation. *J Exp Biol* 205: 2643-2651, 2002.

11. **Cutler CP, Martinez AS, and Cramb G.** The role of aquaporin 3 in teleost fish. *Comp Biochem Physiol* 148A: 82-91, 2007.

12. **Deane EE and Woo NYS.** Tissue distribution, effects of salinity acclimation, and ontology of aquaporin 3 in the marine teleost, silver sea bream (*Sparus sarba*). *Mar Biotech* 8: 1-9, 2006.

13. **Fabra M, Raldúa D, Power DM, Deen PM, and Cerdà J.** Marine fish egg hidration is aquaporin-mediated. *Science* 307: 545, 2005.

14. **Fabra M, Raldúa D, Bozzo MG, Deen PM, Lubzens E, and Cerdà J.** Yolk proteolysis and aquaporin-1o play essential roles to regulate fish oocyte hydration during meiosis resumption. *Dev Biol* 295: 250-262, 2006.

15. **Giffard-Mena I, Boulo V, Aujoulat F, Fowden H, Castille R, Charmantier G, and Cramb G.** Aquaporin molecular characterization in the sea-bass (*Dicentrachus labrax*): the effect of salinity on AQP1 and AQP3 expression. *Comp Biochem Physiol* 148A: 430-444, 2007.

16. **Gonen T and Walz T.** The structure of aquaporins. *Q Rev Biophys* 39: 361-396, 2006.

17. **Grosell M.** Intestinal anion exchange in marine fish osmoregulation. *J Exp Biol* 209: 2813-2827, 2006.

18. **Hirano T and Mayer-Gostan N.** Eel esophagus as an osmoregulatory organ. *Proc Natl Acad Sci USA* 73: 1348-1350, 1976.

19. **Hirano T, Morisawa M, Ando M, and Utida S.** Adaptive changes in ion and water transport mechanism in the eel intestine. In: *Intestinal Ion Transport*, edited by Robinson JWL. London: Kluwer Academic, 1976, p. 301-317.

20. **Ishibashi K.** Aquaporin subfamily with unusual NPA boxes. *Biochim Biophys Acta* 1758: 989-993, 2006

21. **Hirata T, Kaneko T, Ono T, Nakazato T, Furukawa N, Hasegawa S, Wakabayashi S, Shigekawa M, Chang MH, Romero MF, and Hirose S.** Mechanism of acid adaptation of a fish living in a pH 3.5 lake. *Am J Physiol Regul Integr Comp Physiol* 284: R1199-R1212, 2003.

22. **Jin SY, Liu YL, Xu LN, Jiang Y, Wang Y, Yang BX, Yang H, and Ma TH.** Cloning and characterization of porcine aquaporin 1 water channel expressed extensively in gastrointestinal system. *World J Gastroenterol* 12: 1092-1097, 2006.

23. **Kamsteeg EJ and Deen PM.** Detection of aquaporin-2 in the plasma membranes of oocytes: a novel isolation method with improved yield and purity. *Biochem Biophys Res Commun* 282: 683-690, 2001.

554 24. **Klaren PH, Guzman JM, Reutelingsperger SJ, Mancera JM, and Flik G.** Low salinity
555 acclimation and thyroid hormone metabolizing enzymes in gilthead seabream (*Sparus*
556 *auratus*). *Gen Comp Endocrinol* 152: 215-22, 2007.
557 25. **Kleszczynska A, Vargas-Chacoff L, Gozdowska M, Kalamarz H, Martinez-Rodríguez G,**
558 **Mancera JM, and Kulczykowska E.** Arginine vasotocin, isotocin and melatonin responses
559 following acclimation of gilthead sea bream (*Sparus aurata*) to different environmental
560 salinities. *Comp Biochem Physiol Mol Integr Physiol* 145A: 268-73, 2006.
561 26. **Laemmli UK.** Cleavage of structural proteins during the assembly of the head of
562 bacteriophage T4. *Nature* 227: 680-685, 1970.
563 27. **Laiz-Carrión R, Martín del Río MP, Miguez, JM, Mancera, JM, and Soengas JL.**
564 Influence of cortisol on osmoregulatoin and energy metabolism in gilhead sea beam *Sparus*
565 *auratus*. *J Exp Zool* 298: 105-118, 2003.
566 28. **Laiz-Carrión R, Guerreiro PM, Fuentes J, Canario AV, Martin Del Rio MP, and**
567 **Mancera JM.** Branchial osmoregulatory response to salinity in the gilthead sea bream,
568 *Sparus auratus*. *J Exp Zool* 303A: 563-76, 2005.
569 29. **Lignot JH, Cutler CP, Hazon N, and Cramb G.** Immunolocalisation of aquaporin 3 in the
570 gill and the gastrointestinal tract of the European eel *Anguilla anguilla* (L.). *J Exp Biol* 205:
571 2653-2663, 2002.
572 30. **Ma T and Verkman AS.** Aquaporin water channels in gastrointestinal physiology. *J Physiol*
573 517: 317-326, 1999.
574 31. **Mancera JM, Pérez-Fígares JM, and Fernández-Llebrez P.** Osmoregulatory responses to
575 abrupt salinity changes in the euryhaline gilthead sea bream (*Sparus auratus*). *Comp Biochem*
576 *Physiol* 106A: 245-250, 1993.

32. **Mancera JM, Fernández-Llebrez P, Grondona JM, and Pérez-Fígares, JM.** Influence of environmental salinity on prolactin and corticotropic cells in the euryhaline gilthead sea bream (*Sparus auratus* L.). *Gen Comp Endocrinol* 90: 220-231, 1993.

33. **Mancera JM, Pérez-Fígares JM, and Fernández-Llebrez P.** Effect of cortisol on brackish water adaptation in the euryhaline gilthead sea bream (*Sparus auratus* L.). *Comp Biochem Physiol* 107A: 397-402, 1994.

34. **Mancera JM, Pérez-Fígares, JM, and Fernández-Llebrez P.** Effect of decreased environmental salinity on growth hormone cells in the euryhaline gilthead sea bream (*Sparus auratus* L.). *J Fish Biol* 46: 494-500, 1995.

35. **Mancera JM, Laiz-Carrión R, and Martín del Río MP.** Osmoregulatory action of PRL, GH, and cortisol in the gilthead seabream (*Sparus auratus* L.). *Gen Comp Endocrinol* 129: 95-103, 2002.

36. **Martinez AS, Cutler CP, Wilson GD, Phillips C, Hazon N, and Cramb G.** Regulation of expression of two aquaporin homologs in the intestine of the European eel: effects of seawater acclimation and cortisol treatment. *Am J Physiol Regul Integr Comp Physiol* 288: R1733-R1743, 2005.

37. **Martinez AS, Cutler CP, Wilson GD, Phillips C, Hazon N, and Cramb G.** Cloning and expression of three aquaporin homologues from the European eel (*Anguilla anguilla*): effects of seawater acclimation and cortisol treatment on renal expression. *Biol Cell* 97: 615-627, 2005.

38. **Martinez AS, Wilson G, Phillips C, Cutler C, Hazon N, and Cramb G.** Effect of cortisol on aquaporin expression in the esophagus of the European eel, *Anguilla anguilla*. *Ann N Y Acad Sci* 1040: 395-398, 2005.

39. **Mobasheri A and Marples D.** Expression of the AQP-1 water channel in normal human tissues: a semiquantitative study using tissue microarray technology. *Am J Physiol Cell Physiol* 286: C529-C537, 2004.

40. **Mobasheri A, Airley R, Hewitt SM, and Marples D.** Heterogeneous expression of the aquaporin 1 (AQP1) water channel in tumors of the prostate, breast, ovary, colon and lung: a study using high density multiple human tumor tissue microarrays. *Int J Oncol* 26: 1149-1158, 2005.

41. **Preston GM, Carroll TP, Guggino WB, and Agre P.** Appearance of water channels in *Xenopus* oocytes expressing cell CHIP28 protein. *Science* 256: 385-387, 1992.

42. **Preston GM, Jung JS, Guggino WB, and Agre P.** The mercury-sensitive residue at cysteine 189 in the CHIP28 water channel. *J Biol Chem* 268: 17-20, 1993.

43. **Santos CR, Estêvão MD, Fuentes J, Cardoso JC, Fabra M, Passos AL, Detmers FJ, Deen PM, Cerdà J, and Power DM.** Isolation of a novel aquaglyceroporin from a marine teleost (*Sparus auratus*): function and tissue distribution. *J Exp Biol* 207: 1217-1227, 2004.

44. **Skadhauge E.** The mechanism of salt and water absorption in the instestine of the eel (*Anguilla anguilla*) adapted to waters of various salinities. *J Physiol* 204: 135-158, 1969.

45. **Skadhauge E.** Coupling of transmural flows of NaCl and water in the intestine of the eel (*Anguilla anguilla*). *J Exp Biol* 60: 535-546, 1974.

46. **Sui H, Han BG, Lee JK, Walian P, and Jap BK.** Structural basis of water-specific transport through the AQP1 water channel. *Nature* 414: 872-878, 2001.

47. **Tingaud-Sequeira A, Fabra M, Otero D, and Cerdà J.** Identification and characterization of a novel subfamily of aquaporin-1-related water channels neofunctionalized in oocytes of marine and catadromous teleosts. In: *Proc. 8th Int. Symp Reproductive Physiology of Fish*, edited by Roudaut G, Labbé C and Bobe J. St. Malo, France, 2007, p. 64.

48. **Utida S, Hirano T, Oide H, Ando M, Johnson DW, and Bern HA.** Hormonal control of the intestine and urinary bladder in teleost osmoregulation. *Gen Comp Endocrinol* 16: 566-573, 1972.

49. **van Hoek AN, Wiener MC, Verbavatz JM, Brown D, Lipniunas PH, Townsend RR, and Verkman AS.** Purification and structure-function analysis of native, PNGase F-treated, and endo-beta-galactosidase-treated CHIP28 water channels. *Biochemistry* 34: 2212-2219, 1995.

50. **Watanabe S, Kaneko T, and Aida K.** Aquaporin-3 expressed in the basolateral membrane of gill chloride cells in Mozambique tilapia *Oreochromis mossambicus* adapted to freshwater and seawater. *J Exp Biol* 208: 2673-2682, 2005.

51. **Yakata K, Hiroaki Y, Ishibashi K, Sohara E, Sasaki S, Mitsuoka K, and Fujiyoshi Y.** Aquaporin-11 containing a divergent NPA motif has normal water channel activity. *Biochim Biophys Acta* 1768: 688-693, 2007.

636 **Figure Legends**

637

638 Fig. 1. Structural features and functional properties of SaAqp1a and SaAqp1b. *A*: Schematic
639 diagram of AQP1 monomer showing the 6 transmembrane (TM) domains, the 2 NPA motifs and
640 the Cys site involved in mercurial inhibition. *B*: Amino acid sequence alignment of TM 2 and TM
641 5, and loops B and E involved in the formation of the pore, of human AQP1 (HsAQP1), *Sparus*
642 *aurata* Aqp1a (SaAqp1a) and Aqp1b (SaAqp1b), and *Anguilla anguilla* Aqp1 (AaAqp1) and
643 Aqp1dup (AaAqp1dup). Identical amino acids are indicated in black boxes, while conserved and
644 semi-conserved substitutions are indicated by a double or single dot, respectively. The asterisks
645 indicate the residues Phe^{56}, His^{180} and Arg^{195} (HsAQP1 numbering) of the pore forming region that
646 are conserved among water-selective AQPs, and the arrowhead points the mercury-sensitive Cys
647 site. *C-D*: Immunofluorescence microscopy of *X. laevis* oocytes injected with SaAqp1a (*C*) or
648 SaAqp1b (*D*) cRNAs and incubated with anti-SaAq1a or anti-SaAqp1b antisera, respectively. The
649 arrows point the plasma membrane and the asterisk indicates the oocyte cytoplasm. Sections from
650 water-injected oocytes incubated with either SaAqp1a or SaAqp1b antisera did not show any
651 positive signal (not shown). Bar, 50 μm. *E*: Osmotic water permeability (P_f) of *Xenopus laevis*
652 oocytes expressing SaAqp1a or SaAqp1b. Oocytes were injected with 50 nl of water containing 1
653 ng SaAqp1a cRNA or 2 ng SaAqp1b cRNA, or with 50 nl of distilled water only (control oocytes),
654 48 h prior to the experiments. P_f was calculated from the time course of osmotic swelling of
655 oocytes, previously incubated with or without 0.7 mM $HgCl_2$, in a hypoosmotic medium. Recovery
656 of $HgCl_2$ inhibition was performed by treatment of oocytes with 5 mM β-mercaptoethanol (βME)
657 for 15 min after mercury exposure. Values are means ± SEM (n = 10-15 oocytes) from two
658 representative experiments. In each panel, bars with different superscripts are statistically
659 significant (ANOVA, $P < 0.05$).

660 Fig. 2. Seabream *aqp1a* and *aqp1b* mRNA expression and protein abundance along the entire
661 length of the intestine in SW acclimated fish. *A*: Relative levels of *aqp1a* and *aqp1b* in the
662 duodenun (D), hindgut (H) and rectum (R) determined by qPCR. The levels were normalized to the
663 *18S* gene and are presented as means ± SEM (n = 3 fish). Bars with an asterisk are statistically
664 different (ANOVA, $P < 0.01$). *B*: Western blot of membrane fractions from *X. laevis* oocytes (0.2
665 oocyte equivalents per lane) injected with water (lane 1), SaAqp1a (lane 2) or SaAqp1b (lane 3),
666 and from duodenum (lane D), hindgut (lane H) and rectum (lane R) (20 μg per lane) using the
667 SaAqp1a antisera. Blots were incubated with anti-SaAqp1a (left panel) or with anti-SaAqp1a
668 preadsorbed with the synthetic peptide (right panel). The SaAqp1a reactive band of approximately
669 26 kDa, possibly corresponding to SaAqp1a monomer, is indicated by an arrow. *C*: Western blot of
670 the same protein extracts than in *B* probed with anti-SaAqp1b (left panel) or with anti-SaAqp1b
671 preadsorbed with the immunizing peptide (right panel). The two very close SaAqp1b reactive
672 bands, of approximately 27 and 29 kDa, are indicated by arrows. In *B* and *C*, apparent molecular
673 masses (kDa) are indicated on the left.
674
675 Fig. 3. Immunofluorescence microscopy on paraffin sections from the duodenum (*A* and *B*) and
676 hindgut (*C*) of SW-acclimated seabream (n = 3 fish) after reaction with the SaAqp1a antisera. In *D*
677 (phase contrast) and *E* (epifluorescence) is shown a control section from hindgut incubated with
678 peptide-negated antiserum. The same negative results were obtained with the preimmune serum
679 (not shown). BB, brush border; BV, blood vessel; E, epithelium; GC, goblet cell; L, lumen; RBC,
680 red blood cells. Bars, 100 μm (*A, C and D*), 20 μm (*B*).
681
682 Fig. 4. Immunofluorescence microscopy on paraffin sections from the duodenum (*A*) and hindgut
683 (*B*) of SW-acclimated seabream (n = 3 fish) after reaction with the SaAqp1b antisera. In *C* and

(phase contrast) and *D* (epifluorescence) is shown a control section from hindgut incubated with peptide-negated antiserum. The same negative results were obtained with the preimmune serum (not shown). Note that SaAqp1b reaction in the duodenum and hindgut is very weak (arrows) even after permeabilization of the tissue sections with SDS (see Materials and Methods). BB, brush border; BV, blood vessel; E, epithelium; GC, goblet cell; L, lumen; RBC, red blood cells. Bars, 100 μm (*A-C)*.

Fig. 5. Immunofluorescence microscopy on paraffin sections from the rectum of SW-acclimated seabream (n = 3 fish) after reaction with the SaAqp1a antisera. Panels *B* and *C* correspond to the regions indicated in *A*. In panel *B*, arrows point the apical membrane of enterocytes, whereas the arrowheads indicate lateral membrane. Panel *D* shows a section stained with hematoxilin and eosin showing the enterocytes located at the base of the intervillus pockets. Panels *E* (phase contrast) and *F* (epifluorescence) show a control section incubated with antigen-negated SaAqp1a. The same negative results were obtained with the preimmune serum (not shown). BB, brush border; GC, goblet cell; L, lumen; RE, rectal epithelium; N, nucleus of enterocytes. Bars, 100 μm (*E* and *F*), 50 μm (*A* and *E*), 20 μm (*B-D*).

Fig. 6. Immunofluorescence microscopy on paraffin sections from the rectum of SW-acclimated seabream (n = 3 fish) after reaction with the SaAqp1b antisera. Panels *B* and *C* correspond to the regions indicated in *A*. Panels *D* (phase contrast) and *E* (epifluorescence) show a control section incubated with antigen-negated SaAqp1b. The same negative results were obtained with the preimmune serum (not shown). BB, brush border; GC, goblet cell; L, lumen; RE, rectal epithelium; N, nucleus of enterocytes. Bars, 50 μm (*A, D* and *E*), 20 μm (*B* and *C*).

Fig. 7. Effect of freshwater acclimation on SaAqp1a abundance in the duodenum, hindgut and rectum. *A*: Representative Western blot of protein extracts (20 μg) of total membranes from different parts of the intestine from 6 fish maintained in seawater (SW) or acclimated in freshwater (FW) for 10 days. Three separate membranes, for duodenum, hindgut and rectum, respectively, each containg protein extracts from SW- and FW- acclimated fish, were exposed to X-ray films for different times to optimize the signal intensity. *B*: Quantitative analysis of intestinal SaAqp1a protein expression from data shown in A. Values are means ± SEM ($n = 6$). Data of FW-acclimated fish with asterisks are significantly different from those of SW-acclimated fish (Student's *t* test; *, $P < 0.05$; **, $P < 0.01$).

Fig. 8. Effect of freshwater acclimation on SaAqp1b abundance in the duodenum, hindgut and rectum. *A*: Representative Western blot of protein extracts (20 μg) of total membranes from different parts of the intestine from 6 fish maintained in seawater (SW) or acclimated in freshwater (FW) for 10 days. Western blots were carried out as described in Fig. 7. *B*: Quantitative analysis of intestinal SaAqp1b protein expression from data shown in A. Values are means ± SEM ($n = 6$). Data of FW-acclimated fish with an asterisk are significantly different from those of SW-acclimated fish (Student's *t* test; *, $P < 0.05$).

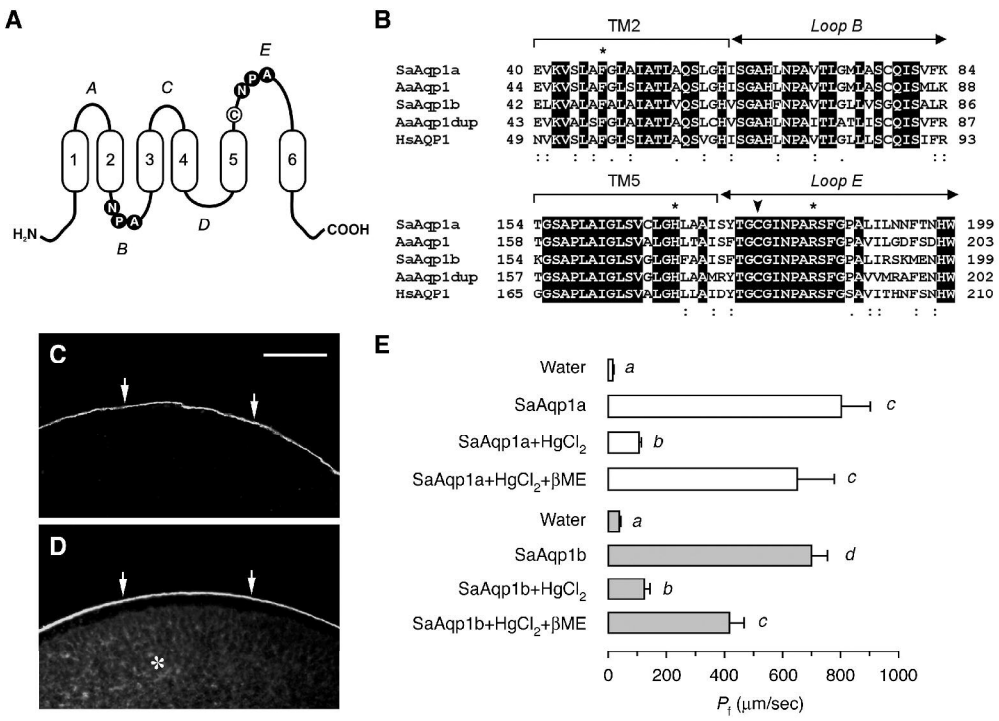

160x115mm (600 x 600 DPI)

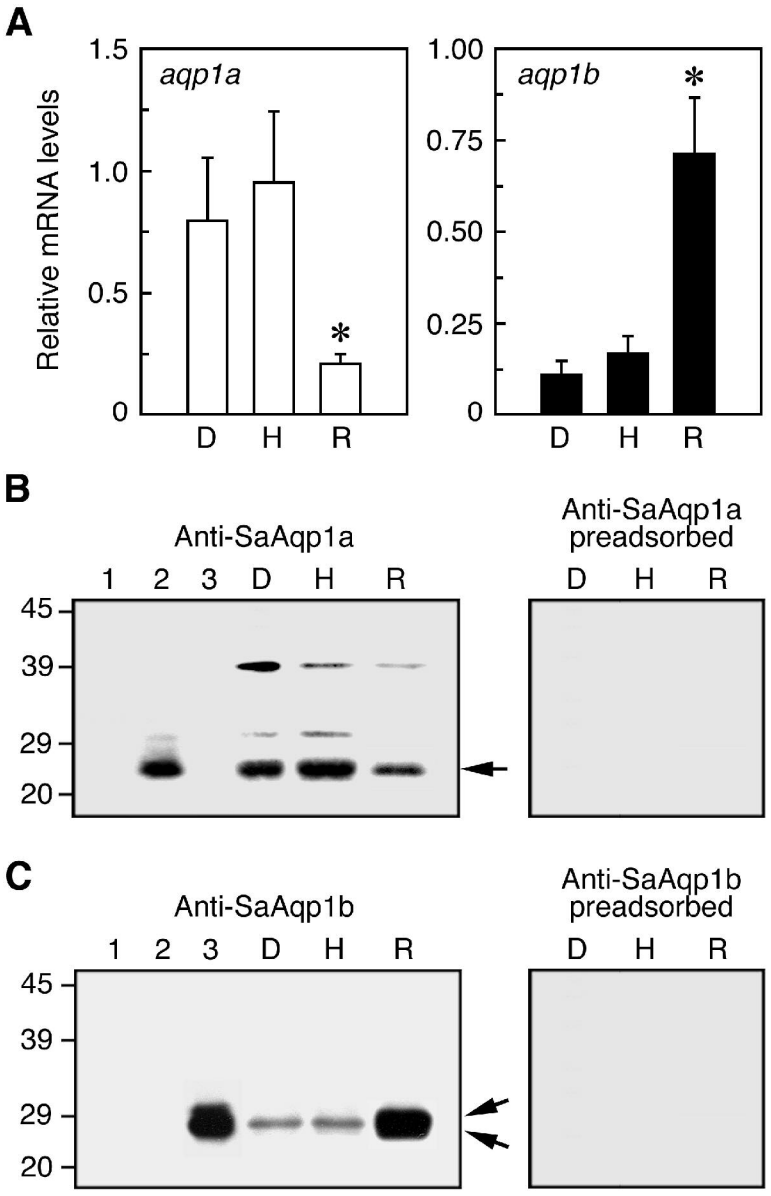

78x123mm (600 x 600 DPI)

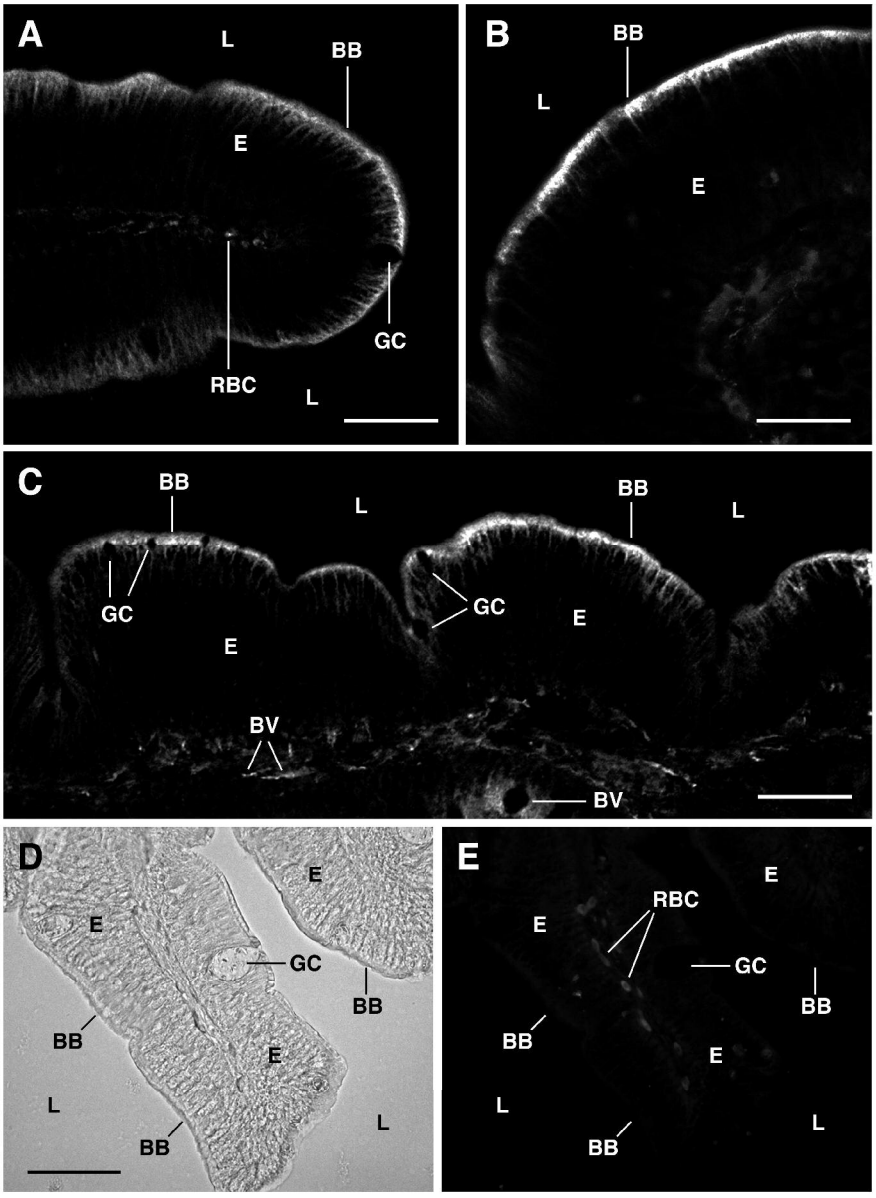

122x165mm (600 x 600 DPI)

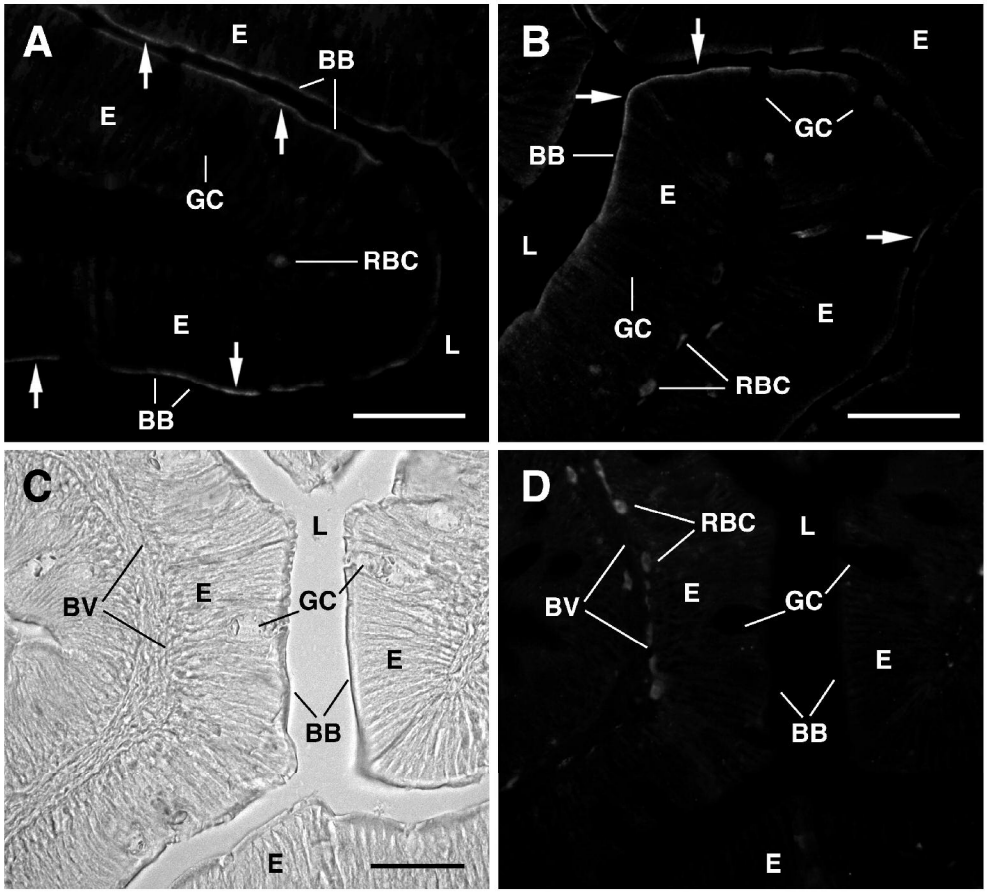

115x104mm (600 x 600 DPI)

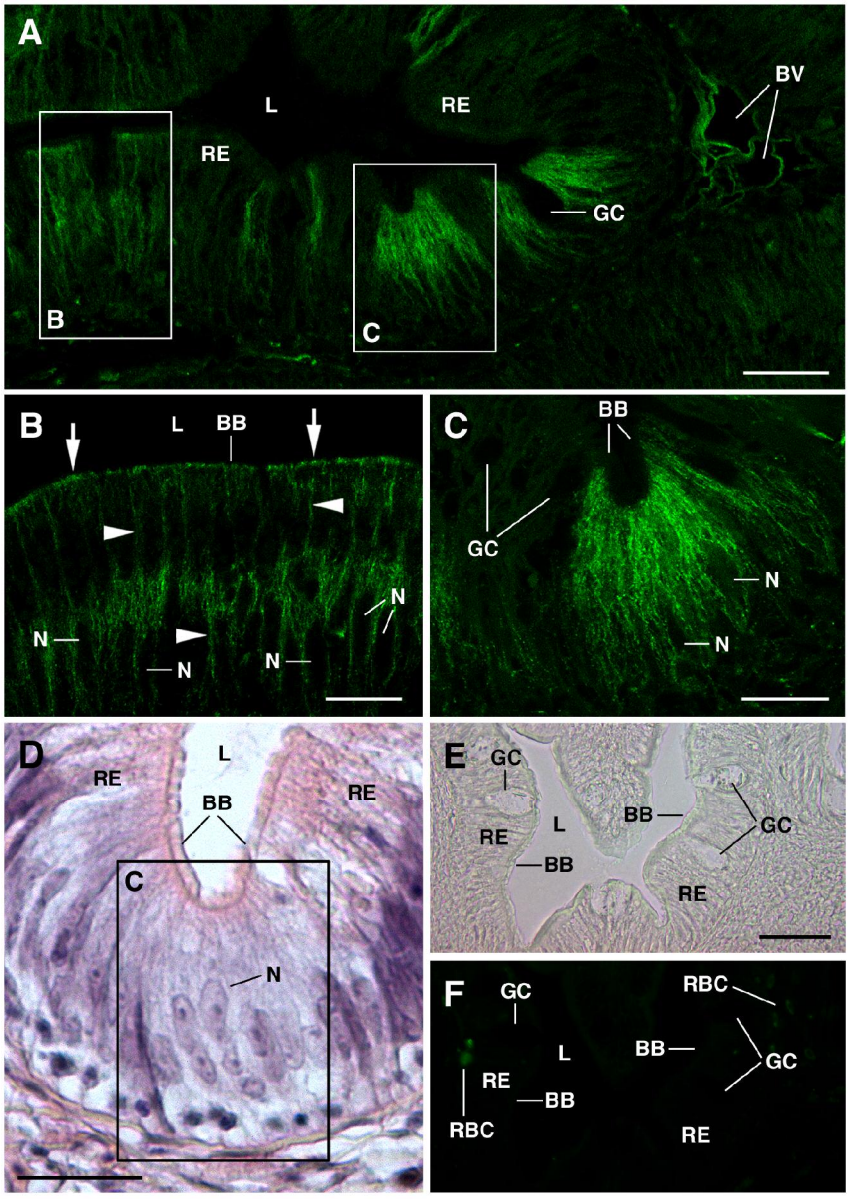

122x171mm (300 x 300 DPI)

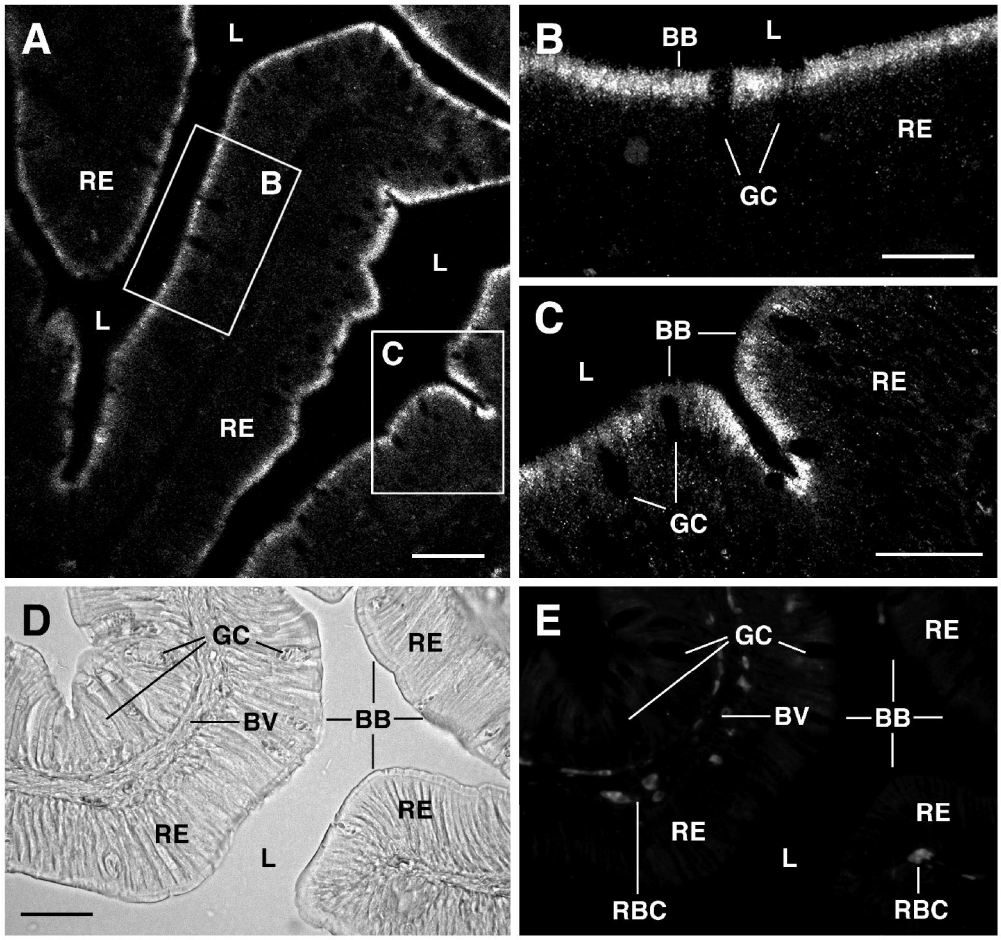

117x109mm (600 x 600 DPI)

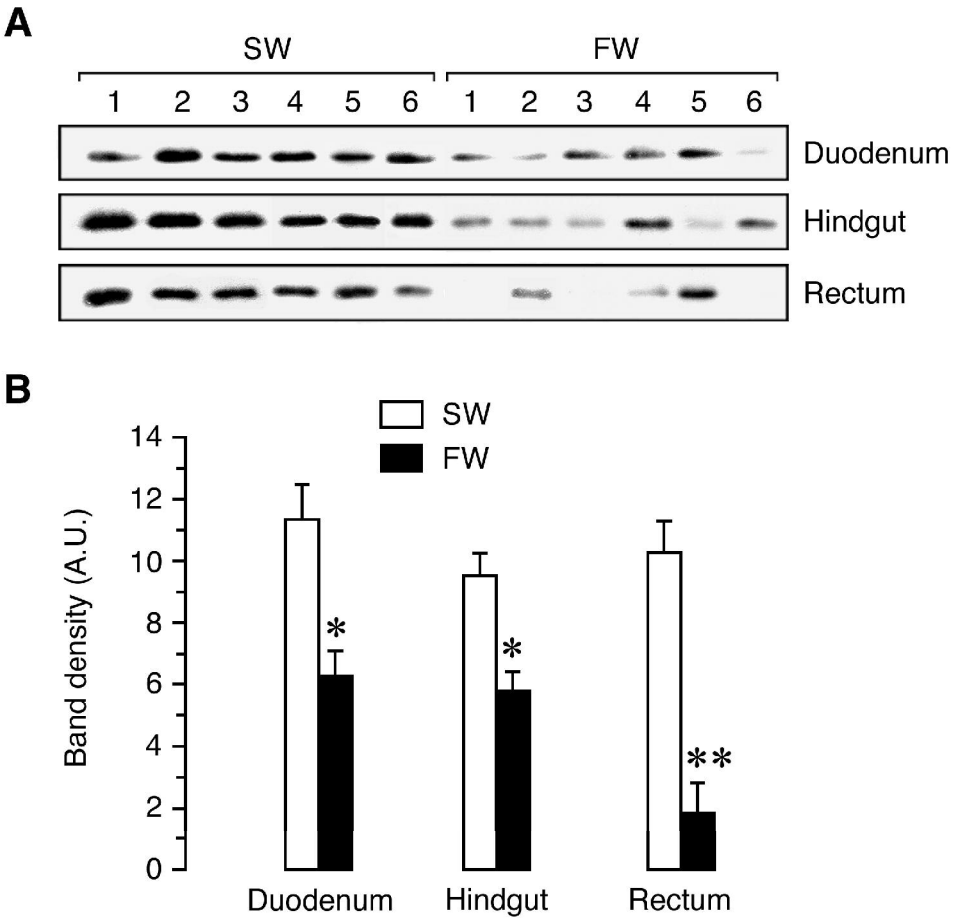

99x99mm (600 x 600 DPI)

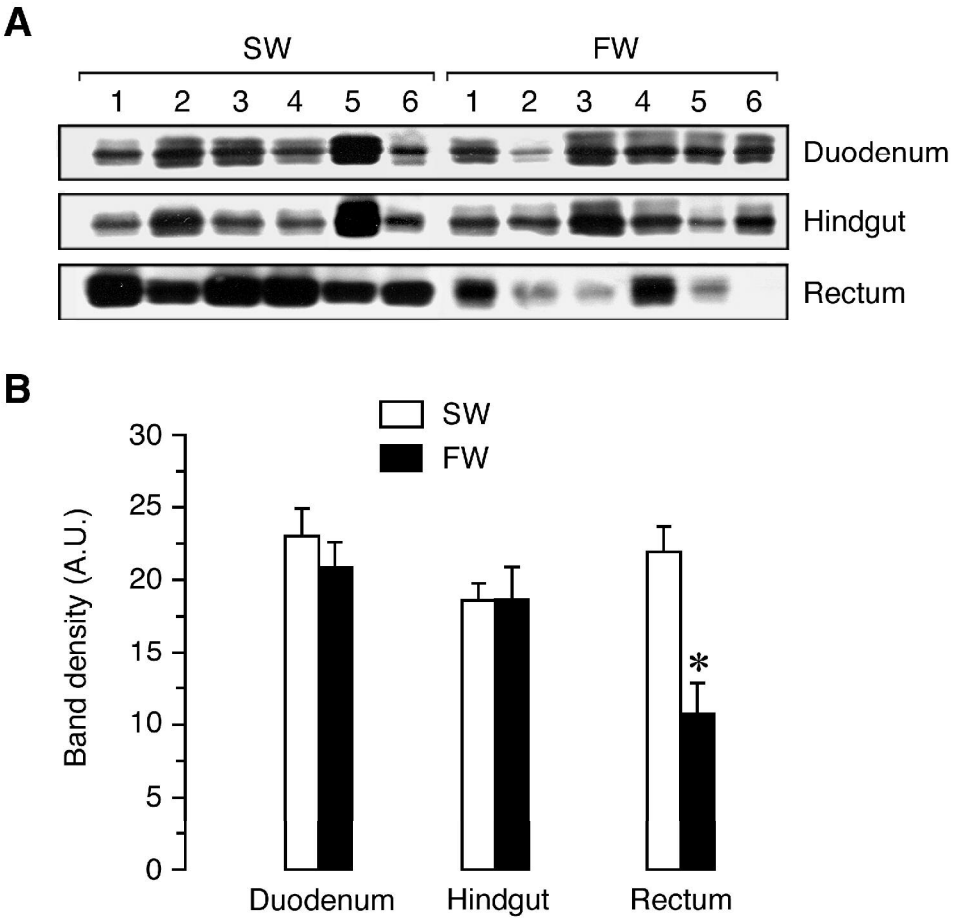

99x99mm (600 x 600 DPI)